

Metallurgy of Friction Welding of Porous Stainless Steel-Solid Iron Billets

S. D. El Wakil

Abstract—The research work reported here was aimed at investigating the feasibility of joining high-porosity stainless steel discs and wrought iron bars by friction welding. The sound friction-welded joints were then subjected to a metallurgical investigation and an analysis of failure resulting from tensile loading. Discs having 50 mm diameter and 10 mm thickness were produced by loose sintering of stainless steel powder at a temperature of 1350 °C in an argon atmosphere for one hour. Minor machining was then carried out to control the dimensions of the discs, and the density of each disc could then be determined. The level of porosity was calculated and was found to be about 40% in all of those discs. Solid wrought iron bars were also machined to facilitate tensile testing of the joints produced by friction welding. Using our previously gained experience, the porous stainless steel disc and the wrought iron tube were successfully friction welded. SEM was employed to examine the fracture surface after a tensile test of the joint in order to determine the type of failure. It revealed that the failure did not occur in the joint, but rather in the porous metal in the area adjacent to the joint. The load carrying capacity was actually determined by the strength of the porous metal and not by that of the welded joint. Macroscopic and microscopic metallographic examinations were also performed and showed that the welded joint involved a dense heat-affected zone where the porous metal underwent densification at elevated temperature, explaining and supporting the findings of the SEM study.

Keywords—Fracture of friction-welded joints, metallurgy of friction welding, solid-porous structures, strength of joint.

I. INTRODUCTION

POWDER metallurgy is gaining wide industrial acceptance because of its capability to produce controlled and unique structures. There is currently, however, a need necessitated by modern industry to expand this capability by joining sintered porous parts to one another, or to wrought parts, in order to form complex solid-porous structures with potential applications in noise abatement and vibration damping. But, since sintered porous and wrought parts have different physical and mechanical properties, welding them together poses several challenges. One possible solution was to employ friction welding, and some work emphasizing the practical aspects of the process has been published [1]–[4]. The current work is a part of a long-term investigation that is aimed at studying all aspects of the friction welding of sintered porous parts to wrought metal components. In the first phase of this investigation, the feasibility of the friction welding of porous and solid metals was proven and was reported in a previous

published work [5], and an understanding of the effects of the various processing parameters was also achieved. Nevertheless, the scope of that study was limited to friction welding of sintered iron compacts to wrought-iron billets, where the base metal in both components was the same, i.e. pure iron. Also, the level of porosity in the sintered porous parts was relatively low (about 15%) making its plastic deformation behavior close to that of a wrought metal.

The current phase of investigation is, therefore, aimed at expanding the scope of the previous experimental study by welding dissimilar parent metals and using sintered parts with high porosity level. It is focused on studying the metallurgy of friction – welded bonds, and the fracture and mode of failure of the produced joints.

II. EXPERIMENTAL

A. Materials

The wrought parts used throughout the friction welding experiments were machined from hot rolled bars of high-purity iron (99.99 w/o) supplied by Armco, Inc., Middletown, Ohio (currently AK Steel, Inc., Middletown, Ohio). Each bar was machined to have a total length of 90 mm and a diameter of 25.4 mm, with one end having two flat parallel surfaces to enable the piece to be held by the grips of a tensile testing machine. The other end of the bar was machined to take the form of a tube with an outer diameter of 25.4 mm and a thickness of 1.6 mm, in order to produce a uniform friction welded joint, with each of its segments at the same distance from the axis of the tube. That was because of a phenomenon observed in the previously published work [5], i.e. the width of the heat-affected zone (HAZ) and thus the heat generated during the process were not constant but varied with the distance from the axis of rotation.

In order to produce the stainless steel porous discs, stainless steel powder (type 302/304) with a particle size of 44 micrometers (supplied by Pellets LLC, New York) was used. Since that powder exhibited poor compressibility, intact green compacts could not be obtained by the ordinary compaction method. It was therefore decided to use loose sintering in order to obtain sound porous discs, as previously mentioned in the literature [6]. Each charge of the stainless steel powder was loosely poured into a pure alumina tube after placing the later on an alumina tray. They were then placed inside a sintering furnace (Sentro-Tech., Ohio) for one hour at a temperature of 1350 °C and in an argon atmosphere. Each sintered porous preform was left to cool down to room temperature in the argon atmosphere, thus ensuring that the austenitic phase was stable and actually annealed. After minor

S. D. El Wakil is with the Mechanical Engineering at the University of Massachusetts Dartmouth, Dartmouth 02747 USA (phone: 508-999-8594, fax: 508-999-8881; e-mail: selewakil@umassd.edu).

machining was carried out to adjust the dimensions of each porous disc, its density could then be calculated by measuring its weight and determination of its volume. All the sintered porous discs used throughout the current experiments had about 40 percent porosity.

B. Friction Welding

All friction-welding operations were carried out on a continuous drive 150 kN friction-welding machine (NCT Company, Newington, Connecticut). The processing parameters were selected based on the experience gained during the first phase of the investigation, which was previously published. The friction time was 3 seconds, the friction pressure was 70 MPa, the forge pressure was 140 MPa, and the rotational speed of the machine's spindle was 1,900 rpm. Six friction-welded joints of sintered porous stainless steel-wrought iron billets were successfully produced.

C. Tensile Testing

Five specimens were subjected to tensile testing. A universal hydraulic testing machine Tinius-Olsen was used throughout the experiments. The range of loading was selected to have up to a maximum reading of 55 kN. That was believed to be appropriate for the low load-carrying capacity of the joints tested.

D. Metallography

A welded joint was spared from tensile testing, and was cut on a plane passing through its axis (meridian plane). It was then subjected to standard metallographic procedures for specimen preparation. These involved grinding and polishing, etching with 5 v/o nital solution, washing in distilled water and then in alcohol, and finally drying in a hot air stream. That was followed by a macro structural examination to identify and characterize the deformation and the HAZs. Finally, each of the identified zones was subjected to micro structural examination in order to detect and analyze any changes that might have occurred in the microstructure as a result of the friction welding operation, such as recrystallization, changes in porosity, and grain growth.

E. Scanning Electron Microscopy

Fractography by SEM analysis was carried out for the fractured surface of one of the specimens that was broken as a result of tensile testing. The scanning electron microscope used was JSM-5610 supplied by JEOL Ltd, Tokyo, Japan.

III. RESULTS

A. Tensile Testing

Fig. 1 shows a friction-welded specimen before and after being subjected to tensile testing. As can be seen in the figure, failure did not occur in the welded joint but rather in the porous stainless steel disc at a distance of about 2 mm away from the edge of the wrought iron tube, producing a very rough surface characterizing brittle fracture. In fact, it revealed that the solid iron tubular end penetrated into the porous disc,

allowing some porous stainless steel to intrude into it and block that tube. The results obtained for the load-carrying capacity of the tensile test specimens was, therefore, not an indication of the strength of the friction-welded joint, but of the sintered porous stainless steel. As it is always the case with sintered porous metals, values of the load-carrying capacity showed a scatter around an average of 35 kN. Evidently, that value cannot be used to determine the strength of the friction-welded joint as previously mentioned.



Fig. 1 A friction-welded specimen before and after a tension test

B. Scanning Electron Microscopy

Scanning electron micrograph of the fractured surface of a tensile test specimen is shown in Fig. 2. It is typical of fractured surfaces of sintered powder metallurgical parts. Pores that are triangular and spherical in shape are scattered all over the surface. These shapes of pores result from the surface tension forces as well as grain boundary migration during sintering. The rough spots in that section were caused by tearing of the necks, which took place between powder particles during sintering, as a result of the tensile force. The fractured surface appears grey and dull, and that is attributed to the oxide films which cover the surfaces of the stainless steel particles, and which absorb electrons, thus keeping part of them from being reflected.

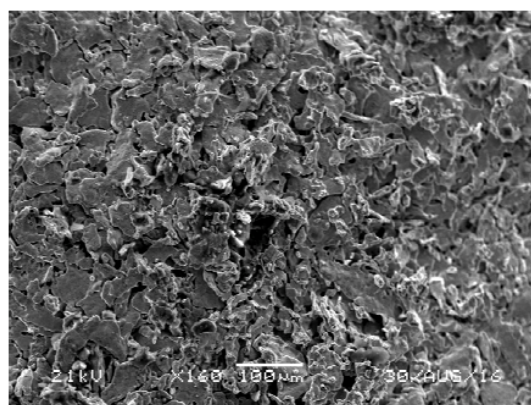


Fig. 2 A scanning electron micrograph of the fractured surface of a test specimen

C. Metallographic Examination

An axial macroscopic section of a friction-welded joint is shown in Fig. 3. The line along which friction welding took place appears as a well-defined trapezoid with a convex base. In fact, it is actually the edge of the wall of the iron tube, which sank into the sintered porous stainless steel disc during the friction welding process, producing an interlocking between those two parts. The heat-affected (HAZ) zone in the sintered porous stainless steel appears as an arch-shaped narrow layer under that trapezoid. Naturally, the picture shows just a cross section, and the HAZ is actually a ring coaxial with the iron tube and having that cross section. The figure also indicates that part of the iron tube was bent inside the tube creating a short thin tube coaxial with the original one.



Fig. 3 An axial macroscopic section of a friction-welded joint

Fig. 4 shows the microstructure of the solid iron tube neighboring the HAZ in the tube. The grains take polygonal shape and are coarse indicating some degree of grain growth as a result of the increase in temperature cause by heat conduction from the HAZ. On the other hand, Fig. 5 shows the microstructure of the solid iron in the HAZ (trapezoid in shape). It has much finer grains than the previous one indicating that recrystallization took place during the friction welding process.

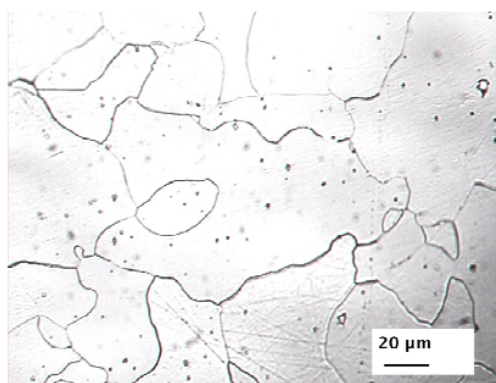


Fig. 4 The microstructure of the solid iron tube neighboring the HAZ

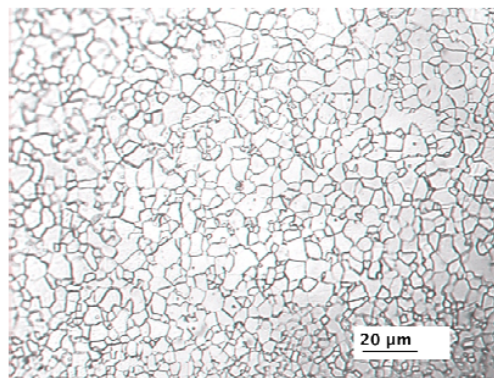


Fig. 5 The microstructure of the solid iron tube in the HAZ

Fig. 6 shows the microstructure of the porous stainless steel disc, whereas Fig. 7 shows the microstructure of the porous stainless steel in the HAZ (HAZ). Since the stainless steel was austenitic, it was resistant to etching, and the grain boundaries could not be revealed. Nevertheless, the shape, size, and distribution of the pores were evident in both figures, and appeared as dark spots. It can be seen in Fig. 6 that the pores have irregular and triangular in shapes and cover a sensible area of the cross section. On the contrary, the pores in the HAZ of the stainless steel (shown in Fig. 7) appear to have been diminished in size due to densification and they are more spherical in shape.

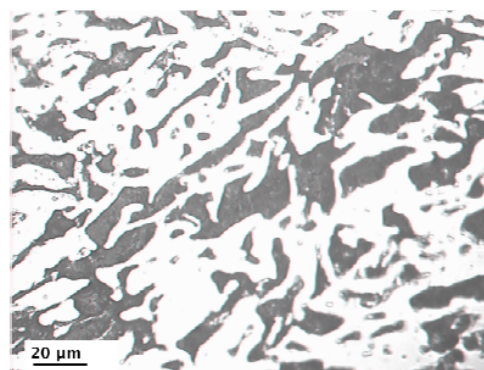


Fig. 6 The microstructure of the porous stainless steel disc

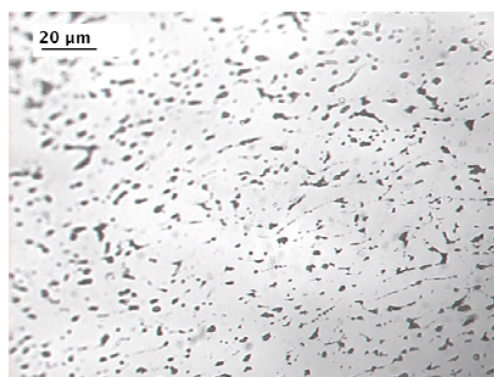


Fig. 7 The microstructure of the porous stainless steel in the heat affected zone

IV. DISCUSSION

As well known, the process of friction welding involves two stages; namely the friction stage and the upsetting stage. The friction stage is aimed at heating the mating surfaces and the neighboring layers to a temperature high enough to enable welding of the two surfaces when the forging pressure is applied during the upsetting stage. Evidently, the heat generated and the rise in temperature caused the recrystallization that took place in the HAZ at the edge of the iron tube during the friction stage. Also, that edge softened as a result of the high temperature and therefore underwent upsetting when the forging pressure was applied. It then penetrated into the porous stainless steel disc producing a very strong joint as a result of both welding and interlocking between the iron tube edge and the stainless steel disc. Meanwhile, diminishing of the pores and densification occurred in the HAZ of the porous stainless steel as a result of the combined action of high temperature and pressure, with the final outcome being strong porous stainless steel in the area. In fact, that explains the mode of failure experienced during the tensile testing of the friction-welded joint, where brittle fracture occurred in the high-porosity stainless outside both the HAZ of the stainless steel and the interface of the welded joint. In fact, that finding is very useful in the design of the configuration of friction welded joints. Components composed of highly porous and solid parts of different parent metals can be produced by friction welding, thus expanding the range of powder metallurgical parts, which have controlled unique structures.

V. CONCLUSION

1. The feasibility of friction welding high-porosity sintered powder preforms to wrought metal components, even when the parent metals are dissimilar, has been demonstrated. High-porosity stainless steel discs were successfully friction welded to wrought iron tubes.
2. The friction welding process had no effect on the porosity of the stainless steel disc, except in the narrow heat – affected zone just under the weld line interface where marked densification took place.
3. The softer metal, i.e. wrought iron underwent plastic deformation because of the forging pressure applied and the rise in temperature. Upsetting of the edge of the tube was evident and the metallographic examination revealed recrystallization. This has to be taken into consideration when designing friction-welded joints.

ACKNOWLEDGMENT

The author would like to thank the following colleagues in the University of Massachusetts Dartmouth for helping with the experimental work: Dan Ducharme, Andrew Smart, Jeffrey Beaudry, and Dr. Chen Lu Yang. Acknowledgment must also go to Enes Serdarvic for helping with the metallography and for Andrew Starczewski who operated the friction welding machine in all the experiments.

REFERENCES

- [1] D. Kluge and U.E. Eckardt, "Schweißen der Werkstoffkombination pulvergeschmiedeter Teile mit Walzblechen", *Schweisstechnik*, vol.36, no. 4, pp.168-170, 1986.
- [2] J. A. Hamill Jr., "What are the Joining Processes Materials and Techniques for Powder Metal Parts?", *International Journal of Powder Metallurgy*, vol. 27, no., pp.363-369, 1991.
- [3] J. P. Hinrichs, P. W. Ramsey and M.W. Zimmerman, "Joining Sintered Steel to Wrought Steel Using Various Welding Processes", *Welding Journal*, vol.50, no.6, pp. 242-246, 1971.
- [4] K. Jayabharath, M. Ashfaq, P. Venugopal and D.R.G. Achar, "Investigations on the Continuous Drive Friction Welding of Sintered Powder Metallurgical (P/M) Steel and Wrought Copper Parts", *Materials Science and Engineering A454*, pp.114-123, 2007.
- [5] S.D. El Wakil, "Friction Welding of Sintered Iron Compacts to Wrought Iron", *International Journal of Powder Metallurgy*, vol.50, no. 4, pp.55-59, 2014.
- [6] S.D. El Wakil and H. Khalifa, "Cold Formability of Billets by Loose Powder Sintering", *International Journal of Powder Metallurgy*, vol.19, no.1, pp.21-27, 1983.